LONDON, METEOROLOGICAL OFFICE.

Met.O. 19 Branch Memorandum No.12.

Determination of the optimum field of view and spacing between observations for a satellite-borne scanning radiometer observing the stratosphere. By CAMPBELL,S. and MAY,B.R.

London,Met.Off.,Met.O.19 Branch Mem.No.12, [1974],31cm.Pp.8,pls.4.Abs.p.1.

Met O 19 Branch Memorandum (No 12)

Determination of the optimum field of view and spacing between observations for a satellite-borne scanning radiometer observing the stratosphere

S Campbell and B R May

HA/EQ/13

DETERMINATION OF THE OPTIMUM FIELD OF VIEW AND SPACING BETWEEN OBSERVATIONS FOR A SATELLITE-BORNE SCANNING RADIOMETER OBSERVING THE STRATOSPHERE

by S Campbell and B R May

Abstract:

Calculations have been made of the optimum size of the field of view and the spacing between observations to be made by an infra-red scanning radiometer observing the stratosphere. The method used is to minimise the rms difference between the true radiance field and observed radiances calculated from the true radiances, account being taken of the instrumental noise. The calculations have been made for a practical range of achievable instrumental noises.

1. Introduction

Considerable advances have been made in the last few years in the field of remote sensing of the Earth's atmosphere by radiometers mounted on orbiting spacecraft. In particular the Selective Chopper Radiometer (SCR) on the Nimbus 4 spacecraft designed by staff of the Atmospheric Physics Department of the University of Oxford, and of Reading University has been very successful in demonstrating the possibility of making continuous radiometric measurements of the stratosphere to deduce its vertical and horizontal temperature structure.(Nature 228,139(1970)).

In 1977 NASA plan to launch the first of the TIROS N series of operational spacecraft. Each will contain, along with other radiometers, a Stratospheric Sounder Unit (SSU) to be supplied by the Meteorological Office. The work described here has been carried out in connection with the design of the SSU and its purpose is to determine the optimum viewing cone angle and the number of observations per scan to be made by a scanning radiometer observing the stratosphere. Although the calculations have been made specifically for the SSU, the principle of the method is quite general and could be adopted for radiometers in different orbits or with different instrumental noise characteristics.

2. The TIROS N spacecraft and the operation of the SSU

The TIROS N spacecraft is planned to travel in a near-polar circular orbit

with a mean height of 833km and a period of 101.6 minutes, so that successive tracks of the satellite are displaced 25.4° westward in longitude. The SSU scans the atmosphere across the sub-spacecraft track with a movement of the viewing cone of constant angular increments, spending a negligible time moving from one observation direction to the next and from the end of one scan to the beginning of the following one. The scan covers an angle of 39° on either side of the nadir resulting in the observations being confined to an area on the ground approximately 1400 km wide centred on the track. This is half the spacing between orbits near the equator so that two spacecraft are planned for the operational system, each spacecraft making observations in the gaps left by the other one. At high latitudes there is a considerable degree of overlap of the observations made on successive orbits but the optimum viewing conditions determined here are for the equatorial regions.

For simplicity it is assumed that during each scan the spacecraft is stationary and then moves forward for the next scan; also that close to the track the distances between the observations along and across the track are the same. If the radiometer makes N observations in the 78° scan, then close to the track the distance between the observations is

$$S = 1133/N \text{ km} \qquad \ldots\ldots\ldots\ldots\ldots\ldots (1)$$

The sub-spacecraft point moves at 6.6 km $.sec^{-1}$ so that the times available for each scan, T, and for each observation, t, are S/6.6 secs and $S/(6.6 \times N)$ respectively (it is assumed that the radiometer makes the observations in the three channels simultaneously). Thus

$$T = 171/N \qquad \ldots\ldots\ldots\ldots\ldots\ldots (2)$$

and $$t = 171/N^2 \text{ seconds} \qquad \ldots\ldots\ldots\ldots\ldots\ldots (3)$$

The radiometer has a circular viewing cone of angle θ which projects onto the ground close to the track a circle of diameter D given by

$$D = \theta \times 14.6 \text{ km} \qquad (\theta \text{ in degrees}) \qquad \ldots\ldots\ldots\ldots (4)$$

3. Instrumental noise of the radiometer

The radiometer to be used in the SSU is the pressure-modulated radiometer (PMR). According to K H Stewart (private communication) the rms noise of this type of

radiometer, which is governed by the detector and optical system, is proportional to

$$(89.6 + 0.038\,\Theta^2)^{\frac{1}{2}}/\Theta^2 \qquad (\Theta \text{ in degrees})$$

For the range of values of Θ within which the optimum values lie, the second term in the brackets is about 10% of the first and is neglected. The time duration of the observations also governs the rms noise which is proportional to $t^{-\frac{1}{2}}$. Combining these two factors, the rms noise of observations is given by

$$\sigma(n_I) = \sigma(n_I^*) \cdot \Theta^{-2} \cdot t^{-\frac{1}{2}} \qquad \ldots\ldots\ldots\ldots(5)$$

where $\sigma(n_I)$ is the rms instrumental noise expressed in radiance units (R.Us - ergs. $sec^{-1} cm^{-2} . sr^{-1} (cm^{-1})$), $\sigma(n_I^*)$ is the "normalised" instrumental noise in I units (I units - R.U. $sec^{\frac{1}{2}} deg^2$) which a radiometer would have if it made one-second observations with a one-degree viewing cone.

From a study of the P.M.R, J T Houghton (private communication) has suggested that it is possible to achieve an rms noise of 0.2° K (equivalent to 0.26 R.U. for a mean radiance of 85 R.U. and a wavenumber of $669 cm^{-1}$) with t = 6 seconds and $\Theta = 10^\circ$. This corresponds to a value of $\sigma(n_I^*) = 65$ I units, but values from 0 to 150 I units were used to investigate the effect of changing the achievable instrumental noise.

4. Calculation of $\sigma(\Delta R)$ as a function of N and Θ

It is assumed that the fidelity with which a noisy radiometer observes a field of atmospheric radiance is measured by $\sigma(\Delta r)$, the rms deviation of the true and observed radiances, which consists of two components. The first component $\sigma(\Delta R)_{atm}$ is caused by the smoothing effect of the finite size field of view and distance between observations on the atmospheric radiance field; the second component $\sigma(\Delta R)_{ins}$ is caused by the instrumental noise and is directly proportioned to $\sigma(n_I^*)$. $\sigma(\Delta R)_{atm}$ and $\sigma(\Delta R)_{ins}$ are both functions of N and Θ which can be determined separately and then combined to find $\sigma(\Delta R)$ using the relationship:-

$$\sigma(\Delta R)^2 = \sigma(\Delta R)^2_{atm} + \sigma(\Delta R)^2_{ins} \qquad \ldots\ldots\ldots\ldots(6)$$

For the purposes of calculating $\sigma(\Delta R)_{atm}$ as a function of N and Θ the true atmospheric radiance field is represented by spot values on a rectangular grid with a 10 km spacing which were obtained in the manner described in the appendix, and the computer is used to simulate the observations that would be made by

the radiometer travelling over the field. The position and outline of the fields of view projected by the viewing cone on the atmosphere are determined for the chosen combination of N and Θ, the increase in both the distance between the observation on the ground and their ellipticity as the cone points more obliquely being correctly represented in the simulation. The true radiances within each field of view are averaged and the resulting means, ascribed to the position of the centre of the fields of view, are used as the observed radiances. For each true radiance gridpoint an estimate of the observed radiance is obtained from the four surrounding values by two-dimensional linear interpolation. From these coincident true and interpolated observed radiances $\sigma(\Delta R)_{atm}$ is calculated.

$\sigma(\Delta R)_{ins}$ can be calculated more directly without using simulation. If the instrumental noise of the observations (which are arranged in a square or rectangular pattern) is $\sigma(n_I)$ then the mean noise at all of the interpolated true radiance grid points is given by

$$\sigma(\Delta R)_{ins} = \sigma(n_I) \times \left(\int_{\alpha=0}^{\alpha=1} ((1-\alpha)^2 + \alpha^2)\, d\alpha \right)^2 = 0.66 \times \sigma(n_I) \qquad \ldots\ldots(7)$$

The factor of 0.66 seems to be reasonable since the [illegible] noise at the observation points is $\sigma(n_I)$ decreasing to $0.5 \times \sigma(n_I)$ midway between four observation points. Thus from equations 3, 5 and 7

$$\sigma(\Delta R)_{ins} = \sigma(n_I^*) \times \frac{0.66}{\sqrt{171}} \times \frac{N}{\Theta^2} \qquad \ldots\ldots(8)$$

$\sigma(\Delta R)_{atm}$ was calculated for combinations of N from 3 to 12 observations per scan and Θ from 2° to 30° in steps of 2°; these were combined with $\sigma(\Delta R)_{ins}$ from equation 8 to calculate $\sigma(\Delta R)$ as a function of N and Θ (using equation 6) for values of $\sigma(n_I^*)$ from 10 to 150 I units.

5. Discussion of results

The spectrum in figure 3 demonstrates that the atmospheric radiance noise (variance) increases rapidly with wavelength so that as Θ increases and N decreases (which increases the scale of the smoothing) $\sigma(\Delta R)_{atm}$ increases. The same change in Θ and N produces a decrease in $\sigma(\Delta R)_{ins}$ in accordance with equation 8. Thus for some particular optimum combination of Θ and N, $\sigma(\Delta R)$ has a minimum value which it is assumed identifies the best representation of the true radiance field by the observation. In figure 1 $\sigma(\Delta R)$ for $\sigma(n_I^*)$ = 65 I units (the value suggested for the PMR) is plotted as a function of N and Θ along with $\sigma(\Delta R)_{atm}$ and $\sigma(\Delta R)_{ins}$. The minimum of $\sigma(\Delta R)$ is not well defined so that N_{opt} and Θ_{opt} are not critically determined, but $\sigma(\Delta R)$

does increase rapidly if $N \gg N_{opt}$ and $\theta \ll \theta_{opt}$ when it is dominated by instrumental noise. For this value of $\sigma(n_I^*)$, $\sigma(\Delta R)_{min.} = 0.10$ R.U., $N_{opt} = 6$ observations per scan corresponding to S = 190 km, t = 4.8 seconds and T = 29 seconds (equations 1, 2 and 3) and $\theta_{opt} = 20^\circ$, equivalent to D = 292 km (equation 4).

If $\sigma(n_I^*)$ is decreased the value of $\sigma(\Delta R)_{min.}$ also decreases in proportion (equation 8) and the minimum in $\sigma(\Delta R)$ is displaced towards larger values of N_{opt} and smaller values of θ_{opt}, resulting in an increase in the resolving power of the radiometer. The variation of $\sigma(\Delta R)_{min.}$, N_{opt} and θ_{opt} with $\sigma(n_I^*)$ from 10 to 150 I units is shown in figure 2; they change more rapidly when $\sigma(n_I^*)$ is small but achieve almost steady values for $\sigma(n_I^*) > 60$ I units. For a noise-free instrument (for which $\sigma(\Delta R) = \sigma(\Delta R)_{min.}$ the dashed lines in figure 1) there appears to be no minimum in $\sigma(\Delta R)$, certainly not within the range of N and θ considered. In the optimum viewing configuration the fields of view always touch or overlap - the ratio $D_{opt} : S_{opt}$ has values of 1.7, 1.0 and 1.5 for $\sigma(n_I^*) = 10$, 60 and 150 I units respectively.

It was mentioned previously that it was assumed for simplicity that the spacecraft remains stationary during a scan and then moves forward for the next scan. Sample calculations were made in which the continuous motion of the spacecraft was simulated giving rise to scans at an oblique angle to the sub-spacecraft track - the difference between the results for the two circumstances was found to be negligible.

Acknowledgement

The authors would like to thank C Morgan of the Clarendon Laboratory, Oxford, for supplying the Nimbus 4 SCR channel A radiances.

Appendix

The determination of suitable values of N and Θ for a radiometer requires a knowledge of the spatial variation of the stratospheric radiance to be measured as explained previously. This variation cannot easily be deduced from rocket temperature-sonde observations due to the small numbers that are made each day (~5). It is possible, though, to use radiance observations directly as made by radiometers already in orbit but remembering that these instruments present a picture of the true spatial variation of radiance modified by their own field-of-view and spacing pattern. The radiances used in this report are those made by the channel A of the Nimbus 4 Selective Chopper Radiometer which has a weighting function peak near 2mb. The field of view of Channel A is a square of side 150 km moving at 6.2 km sec^{-1} at the satellite nadir and the basic observations are one-second means. These observations are processed at the Clarendon Laboratory, Oxford in the following way:

1. Means are taken of 16 successive radiances - call these means R(16).
2. Running means of three successive values of R(16) are then taken four times, equivalent to smoothing R(16) by a weighting function which is roughly Gaussian in shape with a half-width of about 500 km - call these observations R(16)*

These values of R(16)* tabulated each 16 seconds (during which time the field-of-vi moves 100 km) are the observations supplied to the Meteorological Office.

It is assumed that the observations are of a one-dimensional radiance field and so it is possible to estimate the factor by which the amplitude of a sine-wave variation of radiance would be reduced by the field of view and the meaning processes detailed above. The running mean over a length ℓ of a sine wave of wavelength λ also varies sinusoidally and the ratio of the amplitude of the smoothed to the unsmoothed wave is given by $F(\ell/\lambda) = (\sin(2\pi\ell/\lambda))/(2\pi\ell/\lambda)$ (a phase change of π between the two waves may occur depending upon the value of ℓ/λ but it is of no consequence here). Thus the 150 km square field-of-view of channel A causes a reduction by a factor $F(150/\lambda)$ in the apparent amplitude of a wave of length λ km, while the meaning processes (1) and (2) cause a further reduction by factors of $F(100/\lambda)$ and $(F(300/\lambda))^4$ respectively.

The values of R(16)* have been spectrally analysed using a finite Fourier transform embodying the Bartlett lag window applied to the auto-correlation function

in order to smooth the spectrum. An initial investigation of the data showed that the amplitude of the radiances decreased rapidly with frequency so that a high frequency-pass filter was first applied to the data to prevent the spectral engergy at the low frequencies obscuring the detail at the more interesting higher frequencies. The radiances from three complete orbits of the Nimbus D satellite were analysed (roughly 400 values of R(16)* in each) and the results agreed very closely. The results for one of the orbits, starting 0146 UT on 12 December 1970 are shown in figure 3 in which the spectral density S (the variance of the radiance per unit spatial frequency bandwidth in units of $R.U.^2(Km^{-1})^{-1}$) is plotted as a function of the frequency f in Km^{-1}. Scales of wavelength in km and the approximate amplitude in R.Us of the equivalent sine wave are also shown. $Log_{10}(S)$ varies almost linearly with $log_{10}(f)$ for $f < 10^{-3} km^{-1}$ but at higher frequencies the spectrum becomes obscured by instrumental and computational noise. A local minimum of amplitude should be observed at $f = 3.33 \times 10^{-3} km^{-1}$ ($\lambda = 300$ km) due to process 2 mentioned above but this is concealed by the noise (the minima at 150 and 100 km wavelength are not present anyway since the spectrum only extends down to a wavelength of 200 km ($f = 5 \times 10^{-3}$) which is twice the sampling length). The dash-dot line in figure 3 represents the estimated noise-free spectrum obtained by subtracting noise with a spectral density of 2.5 $R.U.^2 (Km^{-1})^{-1}$ from the continuous line. The correction for the finite size of the field of view and the smoothing processes (1) and (2) were then applied resulting in the dashed line in figure 3. For frequencies greater than $1.5 \times 10^{-3} km^{-1}$ the corrections became large and unreliable but the corrected spectrum up to this frequency was smooth and very nearly linear, being well represented by the equation:

$$\log_{10}(S) = 4.1 \log_{10}(f) - 10.8 \qquad \ldots\ldots\ldots\ldots\ldots\ldots (9)$$

(S and f having the units described previously).

This linear spectrum, extended to $f = 0.05\ km^{-1}$ ($\lambda = 20$ km), was used to generate the two-dimensional x-y grid of radiances with a spacing of 10 km referred to in the paper. The radiances were calculated from the equation:

$$R(x,y) = \sum_i A_i \sin(2\pi f_i x + \phi_{xi}) + \sum_i A_i \sin(2\pi f_i y + \phi_{yi}) \quad \ldots\ldots (10)$$

when the f_i are a sequence of centre frequencies spaced at Δf (covering the range 4.5×10^{-5} to $5 \times 10^{-2}\ km^{-1}$) of bands of width Δf, and the A_i are the amplitudes of

sine waves calculated from the variance (amplitude = $\sqrt{2 \times \text{variance}}$) within the frequency bands as given by equation 9. The ϕ_i are random phases.

It should be stressed that the grid of radiances produced by the use of equation 10 only has the required spectrum parallel to the x or y axes. The spectrum of the calculated radiances spaced at 100 km along the x - axis is shown in figure 4 and is in good agreement with the line given by equation 9 which was used to generate the data.

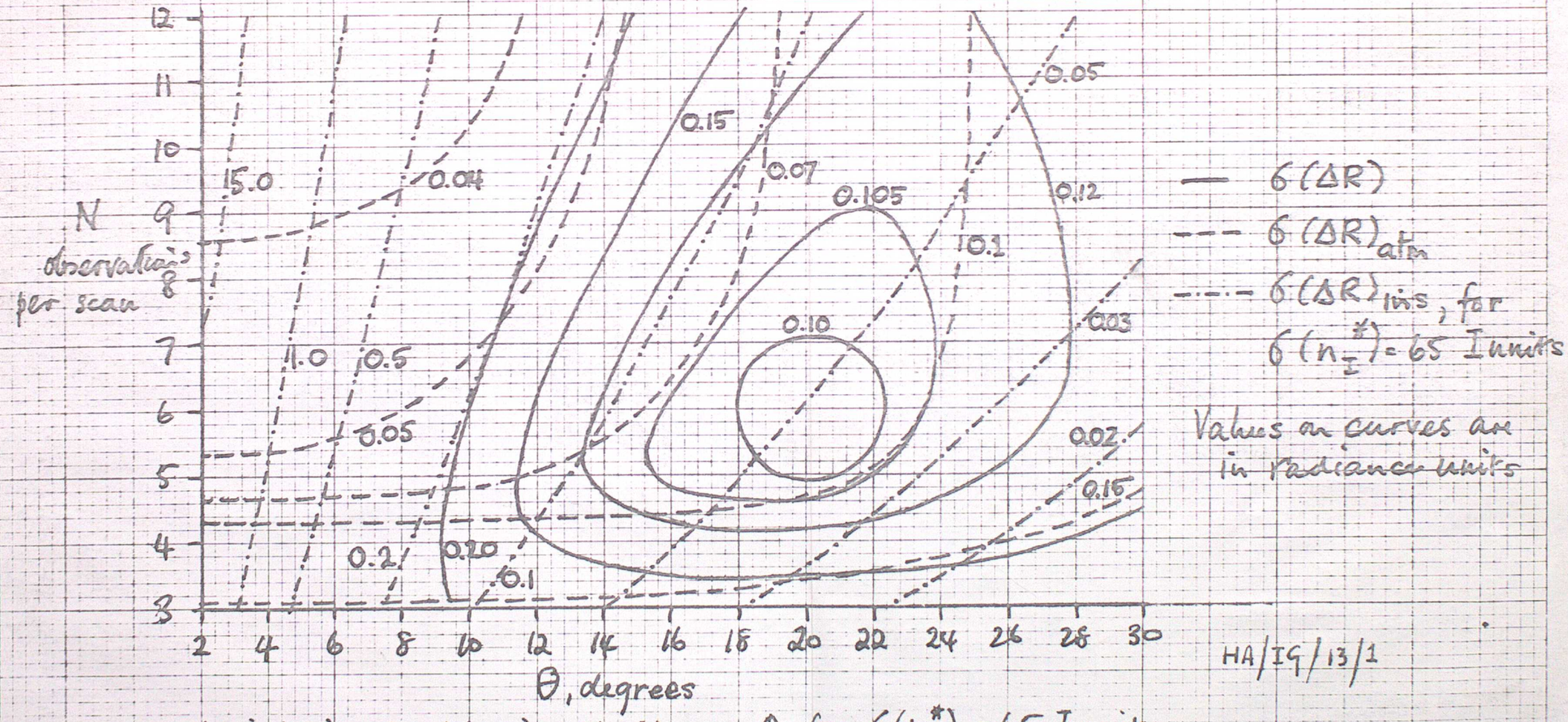

Figure 1 Variation of $\delta(\Delta R)$ with N and θ, for $\delta(n_I^*) = 65$ I units

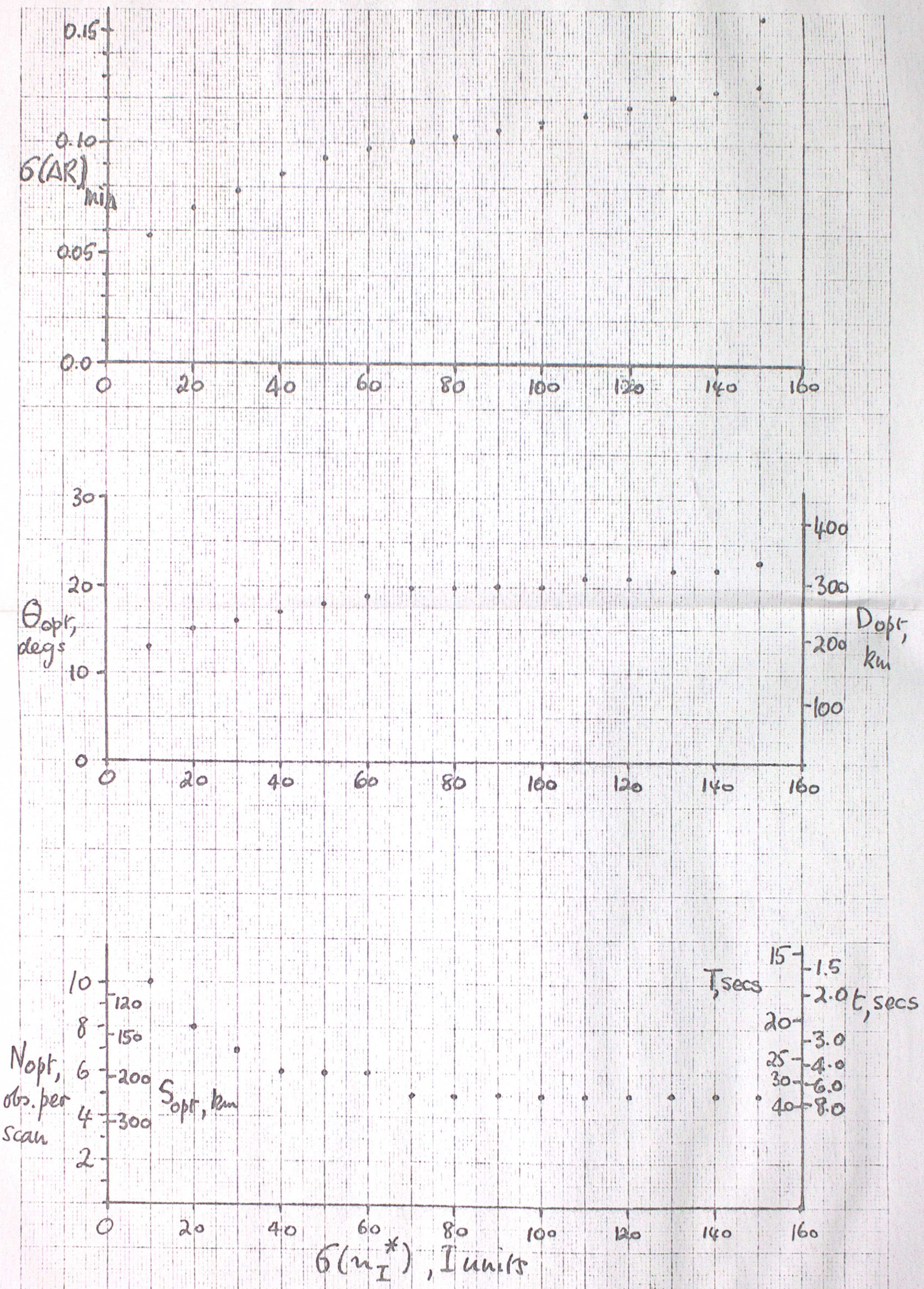

Figure 2 Variation of $\sigma(\Delta R)_{min}$, θ_{opt} and N_{opt} with $\sigma(n_I^*)$

AMPLITUDE, A, IN R.U.

FIGURE 3
SPECTRUM OF NIMBUS 4
SCR CHANNEL A
RADIANCES

CORRECTED FOR
EFFECT OF FINITE
FIELD OF VIEW AND
SMOOTHING OF
RADIANCES

ESTIMATED NOISE
LEVEL

CORRECTED FOR
NOISE

WAVELENGTH, λ, IN KM

FREQUENCY, f, IN KM^{-1}

SPECTRAL DENSITY, S (VARIANCE PER UNIT FREQUENCY BANDWIDTH), IN R.U.^{2}(KM^{-1})$^{-1}$

HA/IG/13/3

AMPLITUDE, A, IN R.U.

10^{2} 10^{1} 10^{0} 10^{-1} 10^{-2}

FIGURE 4
SPECTRUM OF
SIMULATED RADIANCES.

WAVELENGTH, λ, IN KM

10^{5} 10^{4} 10^{3}

SPECTRAL DENSITY, S (VARIANCE PER UNIT FREQUENCY BANDWIDTH), IN $R.U.^2(KM^{-1})^{-1}$

10^{6} 10^{5} 10^{4} 10^{3} 10^{2} 10^{1} 10^{0} 10^{-1}

Equation of line:-

$\log_{10}(S) = -4.1 \log_{10}(f) - 10.8$

10^{-5} 10^{-4} 10^{-3} 10^{-2}

FREQUENCY, f, IN KM^{-1}

HA/IQ/13/+